Room-temperature broadband polariton-lasing from a dye-filled microcavity

Denis Sannikov[1,4], Timur Yagafarov[1], Kyriacos Georgiou[2], Anton Zasedatelev[1,3], Anton Baranikov[1], Lizhi Gai[5], Zhen Shen[5], David Lidzey[2] and Pavlos Lagoudakis[1,3]*

1. Center for Photonics and Quantum Materials, Skolkovo Institute of Science and Technology, Nobelya Ulitsa 3, 121205 Moscow, Russia.

2. Department of Physics and Astronomy, The University of Sheffield, Hicks Building, Hounsfield Road, Sheffield S3 7RH, U.K.

3. Department of Physics and Astronomy, The University of Southampton, University Road, Southampton SO17 1BJ, U.K.

4. The Lebedev Physical Institute of the Russian Academy of Sciences, Moscow, 119333, Russia.

5. State Key Laboratory of Coordination and Chemistry, School of Chemistry and Chemical Engineering, Nanjing University, Nanjing 210046, China

E-mail: D.Sannikov@skoltech.ru

Abstract: We propose a material system to generate polariton lasing at room temperature over a broad spectral-range. The system developed is based on a boron dipyrromethene fluorophore dye (BODIPY-G1) that is dispersed into a polystyrene matrix and used as the active layer of a strongly-coupled microcavity. We show that the BODIPY-G1 exciton-polaritons undergo non-linear emission over a broad range of exciton–cavity mode detuning in the green-yellow portion of the visible-spectrum, with polariton lasing achieved over a spectral range spanning 33 nm. The recorded linewidth of ~0.1 nm corresponds to a condensate coherence lifetime of ~1 ps. We propose that similar effects can be anticipated using a range of molecular dyes in the BODIPY family; a result that paves the way for tuneable polariton devices over the visible and near infrared spectral region.

1. Introduction

Exciton-polaritons have inspired decades of intense interdisciplinary research that has resulted in the emergence of the field of polaritonics; optoelectronics driven on the principle of strong light-matter coupling phenomena.[1] Initial efforts in polaritonics were largely focused on inorganic semiconductor GaAs-based microcavities.[2] However, the applications of III-V and II-VI inorganic semiconductors in polaritonics are relatively limited due to the challenging growth techniques required to create wide-bandgap semiconductors together with the necessity of using cryogenic temperatures to create Mott-Wannier excitons.[3,4]

Organic semiconductors however comprise the broadest class of strongly coupled materials developed to date, and include molecular dyes, crystalline organic molecules, oligofluorenes and conjugated polymers.[5–11] Owing to the high quantum yield, large dipole moment of optical transitions and high binding energy of excitons, organic semiconductors have permitted the physics and applications of polaritonics to be explored at room temperature.[12,13] Polariton lasing is one of the most distinctive nonlinear phenomena related to the collective behaviour of

exciton-polaritons. In contrast to conventional photon lasers, a polariton laser does not necessitate the electronic inversion of population, but is instead driven by a stimulated relaxation to a coherent state during the process of condensation to the ground polariton state. This process has allowed polariton lasers to exhibit significantly lower thresholds compared to photon lasers that have been fabricated using the same device configuration.[14,15]

Recently, we demonstrated polariton lasing in the yellow part of the spectrum in an organic microcavity containing the molecular dye BODIPY-Br.[5] In the present paper, we explore the incorporation of another molecular dye of the BODIPY family, namely BODIPY-G1, into a microcavity, and show that by incorporating a wedged cavity-layer configuration, we can achieve strong-coupling over a broad range of exciton-photon detuning conditions. Such structures allow us to controllably access different cavity lengths and thus select the energy of the ground polariton state. We then use this approach to provide evidence of polariton lasing over a broad range of wavelengths (>30 nm) utilising a single material system.

2. Results and Discussions

We investigate the potential of dye-filled microcavities for broadband tuneable polariton lasers using BODIPY-G1 dye molecules dispersed in a transparent polystyrene matrix as the intracavity material host. The molecular dye BODIPY-G1 is a typical representative of the BODIPY family and combines both high extinction coefficients and high photoluminescence quantum yields.[16] In **Figure 1(a)** we draw a schematic of the microcavity and illustrate the excitation and detection geometry that we implement here. A gradient (up to 10 nm/cm) in the thickness of the cavity region occurs as a result of the spin-casting process results in a broad tunability of exciton-photon detuning conditions (>130 meV). Figure 1(b) shows the normalized absorption and fluorescence spectra measured from a 150 nm thick bare film consisting of BODIPY-G1 dye molecules dispersed into a polystyrene matrix at a concentration

of 10% by mass, spin-cast onto a quartz-coated glass substrate. The absorption maximum occurs at 507 nm with the fluorescence being Stokes-shifted to 524 nm. On a film of the same thickness, we perform amplified spontaneous emission (ASE) measurements, shown in Figure 1(c), that reveal that BODIPY-G1 undergoes optical gain. The maximum of the optical gain spectrum is centred at 547nm as indicated by the narrowing of fluorescence emission at a pump density of ~ 5mJ cm^{-2}. Here, the 150 nm film was excited using a stripe beam excitation using 350 ps laser pulses at a repetition rate of 1 kHz at 355 nm (see Experimental Section). The microcavity was then fabricated by spin-coating a blended film of BODIPY-G1 dispersed into polystyrene onto a distributed Bragg reflector consisting of 10 pairs of SiO_2 / Nb_2O_5. Here the spin-coating process used tended to create films that were slightly thicker at the edge of the substrate. The structure was finally completed by depositing a second 8-pair SiO_2 / Nb_2O_5 distributed Bragg reflector onto the film using ion assisted electron beam and reactive sublimation (see Experimental Section). The dye-filled microcavities created had a cavity Q-factor of ~ 600 (derived from the emission linewidth at normal incidence [$k_{\parallel} = 0$]) and supported strong coupling between the cavity photon and the molecular-exciton resonance. **Figure 2** plots the angular dependence of the reflectivity and demonstrates photon-exciton strong coupling as evidenced by the anti-crossing of the bare modes at ~35˚. The vacuum Rabi energy is 114 meV (see Supporting Information Table S1). The upper and lower polariton branches are observed as local minima in the angular reflectivity plot and undergo an avoided crossing at ~507 nm; a wavelength near the $S_0 \rightarrow S_1$ optical transition of the molecular dye.

To demonstrate polariton lasing, the microcavity was pumped using 2 ps single laser pulses at 400 nm in a transmission configuration (see Figure 1(a)), with polariton emission dispersion recorded for each excitation pulse. **Figure 3(a)** shows the polariton dispersion below (right panel) and above (left panel) threshold at the most negative exciton-photon detuning accessible in our microcavities (-248 meV). Above threshold we observe a collapse of the

photoluminescence to the ground polariton state, accompanied by a line narrowing and a blueshift of the emission. In Figure 3(b) we plot the photoluminescence intensity integrated over ±1 ˚ around normal incidence versus excitation density. At an incident excitation density of ~ 6 mJ/cm^2 we observe a rapid increase of the photoluminescence intensity; a process indicative of a threshold to the non-linear regime. In Figure 3(c) we plot the energy shift (right axis, in blue) and the full width at half maximum of the emission linewidth (left axis, in red) integrated over ±1˚ around normal incidence versus excitation density. At the condensation threshold excitation density, we observe a narrowing of the emission linewidth, and a blue shift of the polariton mode associated with polariton lasing in the strong coupling regime. The tenfold linewidth narrowing from 1 nm to 0.1 nm reflects a high degree of coherence of ~1 ps. The absorbed excitation density at condensation threshold for the BODIPY-G1 here, and BODIPY-Br[5] filled-microcavities is approximately the same.

Having established polariton lasing at the most negative detuning (-248 meV), where the polariton wavefunction is comprised of 4.5% excitonic contribution, we proceeded to examine the full range of exciton-photon detuning in our structures. Here, we recorded almost four hundred observations of polariton lasing across a series of cavity structures spanning the green and yellow parts of the spectrum. **Figure** 4 shows a scatter plot of the emission wavelength of polariton lasing versus detuning. For a subset of these wavelengths we perform the full excitation density dependence that allows us to estimate the threshold for polariton lasing vs exciton-photon detuning. We observe a weak dependence vs detuning with an average threshold of ~ 7 mJ cm^{-2} (standard deviation of 1.5 mJ cm^{-2}). It is worth noting that the absorbed excitation density for polariton lasing is ~ 2.5 times smaller than the excitation density required to reach ASE threshold on a film of the same thickness (for details see Supporting Information). For each data point in Figure 4, we observe the same hallmarks of polariton lasing as shown in Figure 3 (see Supporting Information Figure S1). The black open circles indicate the energy of

the bare cavity mode derived from the measured linear dispersion for each observation of polariton lasing. On the chromaticity diagram of Figure 4, we use a black line to indicate the range of emission-colours in which we obtain polariton lasing with BODIPY-G1.

3. Conclusion

In conclusion, we have demonstrated strong coupling and polariton lasing in microcavities containing the molecular dye BODIPY-G1. By engineering a thickness gradient across the microcavities we have accessed a broad range of exciton-photon detuning conditions. Using these structures, we have shown that BODIPY-G1 can undergo polariton lasing over a broad range (~33 nm) of wavelengths across the green-yellow part of the spectrum, with a highly monochromatic emission line of 0.1 nm. We note that there are a large number of related materials in the BODIPY family having emission that spans visible wavelengths to the near-infrared[17] that are expected to allow polariton lasing to be generated over a similar broad range of wavelengths. We believe that our results pave the way towards coherent lighting applications using strongly coupled organic microcavities. Furthermore, the broad wavelength tunability demonstrated here is of particular interest in the development of hybrid organic-inorganic polaritonics, as it will enable a fine adjustment of the energy separation between various polariton states.

4. Experimental Section

Sample preparation: Polystyrene (PS) having a molecular weight of M_w = 192,000 was dissolved in toluene at a concentration of 35mg/mL to create an optically inert matrix solution. BODIPY-G1 was then dispersed into the solution at 10% by mass. Control films for absorption, photoluminescence and ASE measurements were then spin-cast from solution onto quartz-coated glass substrates.

To fabricate a microcavity, a bottom distributed Bragg reflector (DBR) consisting of 10 pairs of SiO_2/Nb_2O_5 was deposited onto quartz-coated glass substrates using ion assisted electron beam (Nb_2O_5) and reactive sublimation (SiO_2). A BODIPY-G1/PS film was then spin-coated on top of the bottom mirror using 100 μL of solution. Microcavities with different exciton-photon detunings were fabricated by controlling the active layer thickness (ranging from 130 nm to 180 nm) via the substrate rotation speed. A wedge-like thickness gradient within a sample occurred from the spin-coating process. As the casting solution was driven towards the edge of the substrate and evaporated during the process, the remaining polymer-solution increased in viscosity; that resulted in the formation of a thicker film towards the edge of the substrate and allowed us to control an exciton-photon detuning precisely. A second 8-pair DBR was deposited on top of the organic with the ion-gun turned-off during the first few layers to avoid causing damage to the organic material.

Spectroscopy: A Fluoromax 4 fluorometer (Horiba) equipped with a Xe lamp was used to measure the absorption of the BODIPY-G1 control non-cavity films. Films were excited using a 473 nm laser diode and PL was detected using an Oriel MS-125 spectograph. Angular white light reflectivity measurements were performed using an Ocean Optics DH-2000 fibre-coupled Halogen-Deuterium white light source. The angle of incidence between the sample and the white light source was controlled using a motorized arm. The reflected light was coupled into an optical fibre mounted on a second motorized arm which controlled the detection angle. The collected PL was then directed into a Andor Shamrock CCD spectrometer.

ASE measurements were performed using a 355 nm pulsed laser with 350 ps pulse width and 1 kHz repetition rate. A 25 mm cylindrical lens was used to focus the beam on the sample creating a stripe excitation profile (1470 μm x 80 μm). ASE emission from a 150 nm control noncavity film (10% BODIPY-G1 in 35mg/mL PS/toluene) was detected from the edge of the

film, in a direction perpendicular to that of the propagation of the incident pump beam using an Andor Shamrock CCD spectrometer. The laser power at threshold was measured to be P_{th}=6 mW.

To investigate polariton lasing, the microcavities were excited non-resonantly using single 2 ps pulses from a Ti:Sapphire laser (Coherent Libra-HE) which was frequency-doubled through a BBO crystal providing a wavelength of 400 nm. The pump beam was focused onto a sample by Nikon Plan Fluor 4X microscope objective in ~ 12 μm pump spot size at FWHM. Photoluminescence was collected in transmission configuration using Mitutoyo Plan Apo 20X microscope objective with a numerical aperture (NA) of 0.42. To block the residual light from the excitation beam Semrock LP02-442RU longpass filter was used in the collection path. Properly filtered PL of a sample was coupled to 750 mm focal length spectrometer (Princeton Instruments SP2750) equipped with an electron multiplying charge-coupled device camera (Princeton Instruments ProEM-HS 1024X1024). We used 1200 grooves mm^{-1} grating and 20 um entrance slit to achieve a spectral resolution of 0.03 nm. All measurements were performed in air and at room temperature.

Supporting Information

Supporting Information is available from the Wiley Online Library or from the author.

Acknowledgements

This work was supported by the U.K. Engineering and Physical Sciences Research Council (EPSRC) via Progamme Grant EP/M025330/1 (Hybrid Polaritonics), the Skoltech NGP Program (Skoltech-MIT joint project), and the Russian Scientific Foundation (RSF) grant No. 18-72-00227. Denis Sannikov and Timur Yagafarov contributed equally to this work.

Received: ((will be filled in by the editorial staff))
Revised: ((will be filled in by the editorial staff))
Published online: ((will be filled in by the editorial staff))

References

[1] A. V. Kavokin, J. J. Baumberg, G. Malpuech, F. P. Laussy, *Microcavities*, Oxford University Press, New York, US, **2007**.

[2] C. Weisbuch, M. Nishioka, A. Ishikawa, Y. Arakawa, *Phys. Rev. Lett.* **1992**, *69*, 3314.

[3] D. W. Snoke, J. Keeling, *Phys. Today* **2017**, *70*, 54.

[4] D. Sanvitto, S. Kéna-Cohen, *Nat. Mater.* **2016**, *15*, 1061.

[5] T. Cookson, K. Georgiou, A. Zasedatelev, R. T. Grant, T. Virgili, M. Cavazzini, F. Galeotti, C. Clark, N. G. Berloff, D. G. Lidzey, P. G. Lagoudakis, *Adv. Opt. Mater.* **2017**, *5*, 1700203.

[6] C. P. Dietrich, A. Steude, L. Tropf, M. Schubert, N. M. Kronenberg, K. Ostermann, S. Höfling, M. C. Gather, *Sci. Adv.* **2016**, *2*, e1600666.

[7] C. Zhang, C.-L. Zou, Y. Yan, R. Hao, F.-W. Sun, Z.-F. Han, Y. S. Zhao, J. Yao, *J. Am. Chem. Soc.* **2011**, *133*, 7276.

[8] G. G. Paschos, N. Somaschi, S. I. Tsintzos, D. Coles, J. L. Bricks, Z. Hatzopoulos, D. G. Lidzey, P. G. Lagoudakis, P. G. Savvidis, *Sci. Rep.* **2017**, *7*, 11377.

[9] J. A. Torres, R. B. Kaner, *Nat. Mater.* **2014**, *13*, 328.

[10] S. Kéna-Cohen, S. R. Forrest, *Nat. Photonics* **2010**, *4*, 371.

[11] K. S. Daskalakis, S. A. Maier, R. Murray, S. Kéna-Cohen, *Nat. Mater.* **2014**, *13*, 271.

[12] D. G. Lidzey, D. D. C. Bradley, T. Virgili, A. Armitage, M. S. Skolnick, S. Walker, *Phys. Rev. Lett.* **1999**, *82*, 3316.

[13] D. G. Lidzey, D. D. C. Bradley, M. S. Skolnick, T. Virgili, S. Walker, D. M. Whittaker, *Nature* **1998**, *395*, 53.

[14] P. Tsotsis, P. S. Eldridge, T. Gao, S. I. Tsintzos, Z. Hatzopoulos, P. G. Savvidis, *New J. Phys.* **2012**, *14*, 023060.

[15] H. Deng, G. Weihs, D. Snoke, J. Bloch, Y. Yamamoto, *Proc. Natl. Acad. Sci.* **2003**, *100*, 15318.

[16] K. Georgiou, P. Michetti, L. Gai, M. Cavazzini, Z. Shen, D. G. Lidzey, *ACS Photonics* **2018**, *5*, 258.

[17] A. Loudet, K. Burgess, *Chem. Rev.* **2007**, *107*, 4891.

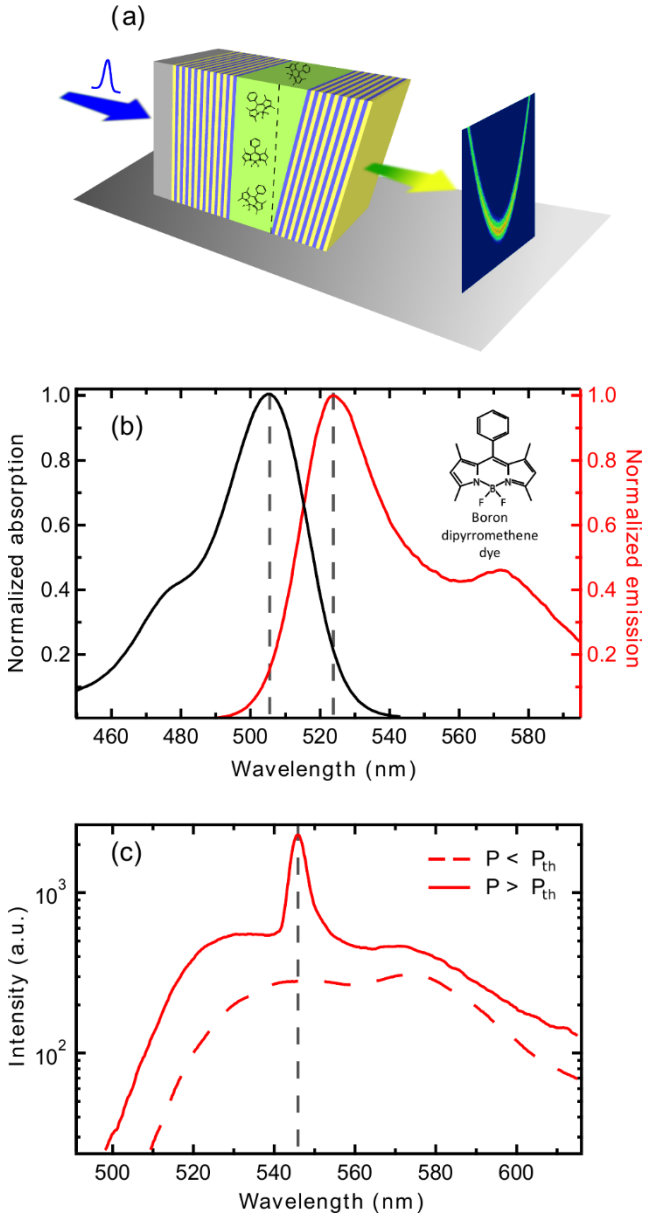

Figure 1 (a) Schematic of the wedged dye filled microcavity and the excitation and detection configuration. (b) Normalised absorption (black) and fluorescence spectrum (red) of a 150 nm thick film of the BODIPY-G1 dye dispersed into a polystyrene matrix. Inset: the chemical structure of BODIPY-G1. (c) Emission spectra of the bare film under stripe beam excitation collected from the side of the sample. The dye molecules undergo amplified spontaneous emission at an incident excitation density of ~ 5mJ/cm^2, with the maximum of the material gain occuring at 547nm.

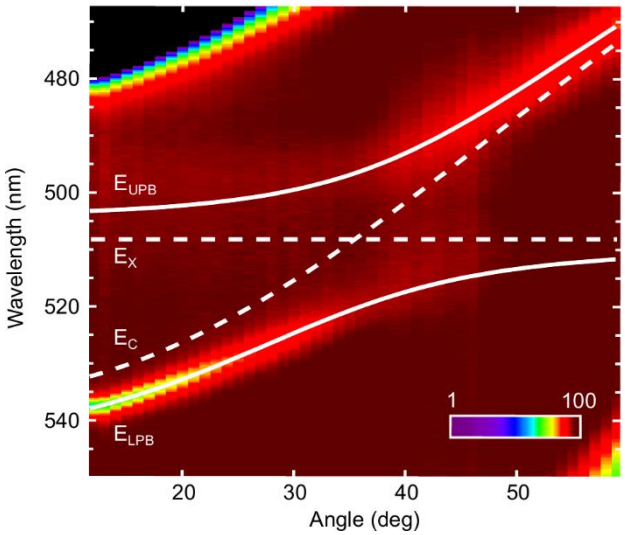

Figure 2 Colour plot of the angle-dependent reflectivity of the BODIPY-G1 filled microcavity (log scale). The solid lines show the calculated upper and lower polariton branches and the dashed lines show the bare cavity and exciton modes. Anti-crossing of the polariton modes is visible at 35˚.

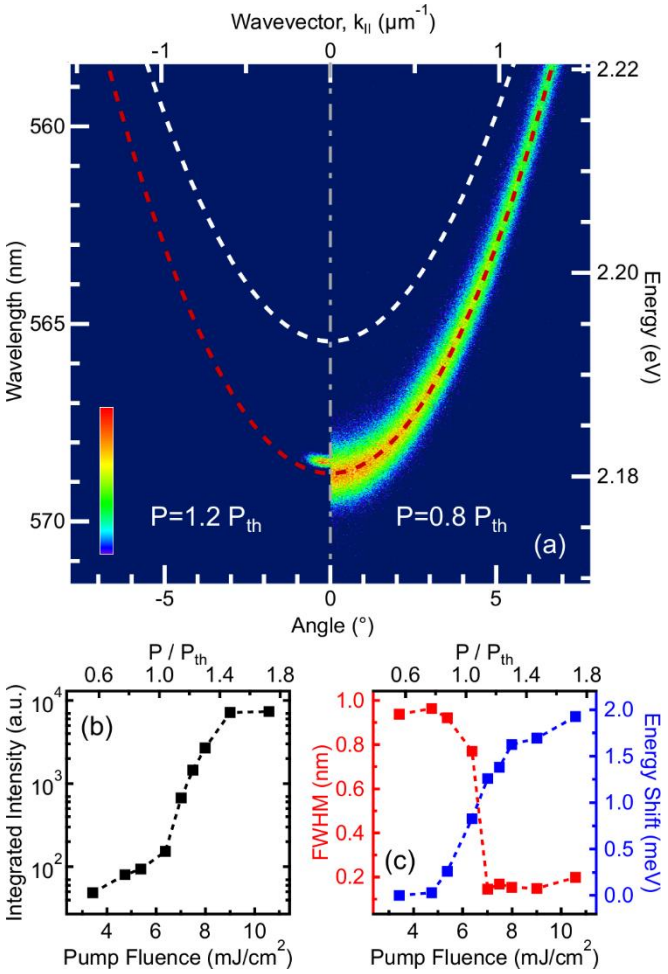

Figure 3 (a) Normalized E, k - dispersion of polariton photoluminescence below (right) and above the threshold (left). The red and white dashed curves indicate the lower polariton branch and the bare cavity mode respectively. (b) The dependence of integrated polariton photoluminescence as a function of pump fluence. (c) The linewidth of polariton photoluminescence at FWHM (red) and the energy shift of the polariton mode at $k_{\parallel} = 0$ (blue) versus pump fluence.

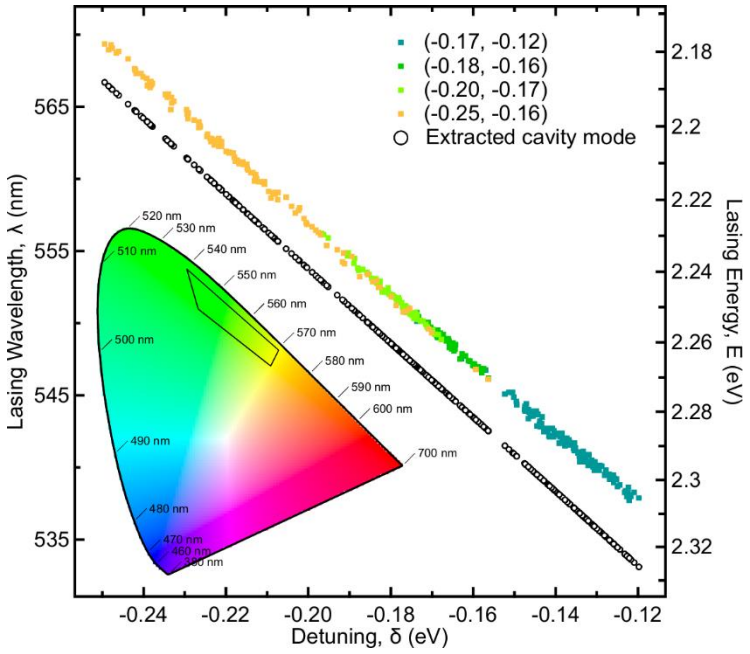

Figure 4 The coloured solid-square data points indicate the wavelength (photon energy – right axis) where polariton lasing was observed versus the corresponding exciton-photon detuning. The black open-circles indicate the corresponding bare cavity mode for each realisation. Polariton lasing spans the green-yellow part of the visible spectrum as indicated with a black solid line on the CIE 1931 chromaticity diagram – bottom left inset.

Keyword: BODIPY-G1, exciton-polaritons, polariton laser, organic microcavity

Supporting Information

Room-temperature broadband polariton-lasing from a dye-filled microcavity

Denis Sannikov[1,4], Timur Yagafarov[1], Kyriacos Georgiou[2], Anton Zasedatelev[1,3], Anton Baranikov[1], Z. Shen[5], David Lidzey[2] and Pavlos Lagoudakis[1,3]

For all realizations of polariton lasing we observe the lasing blue-shifted compared to the bottom of LPB and redshifted with respect to the cavity mode. Figure S1 shows polariton lasing across the whole spectrum studied here.

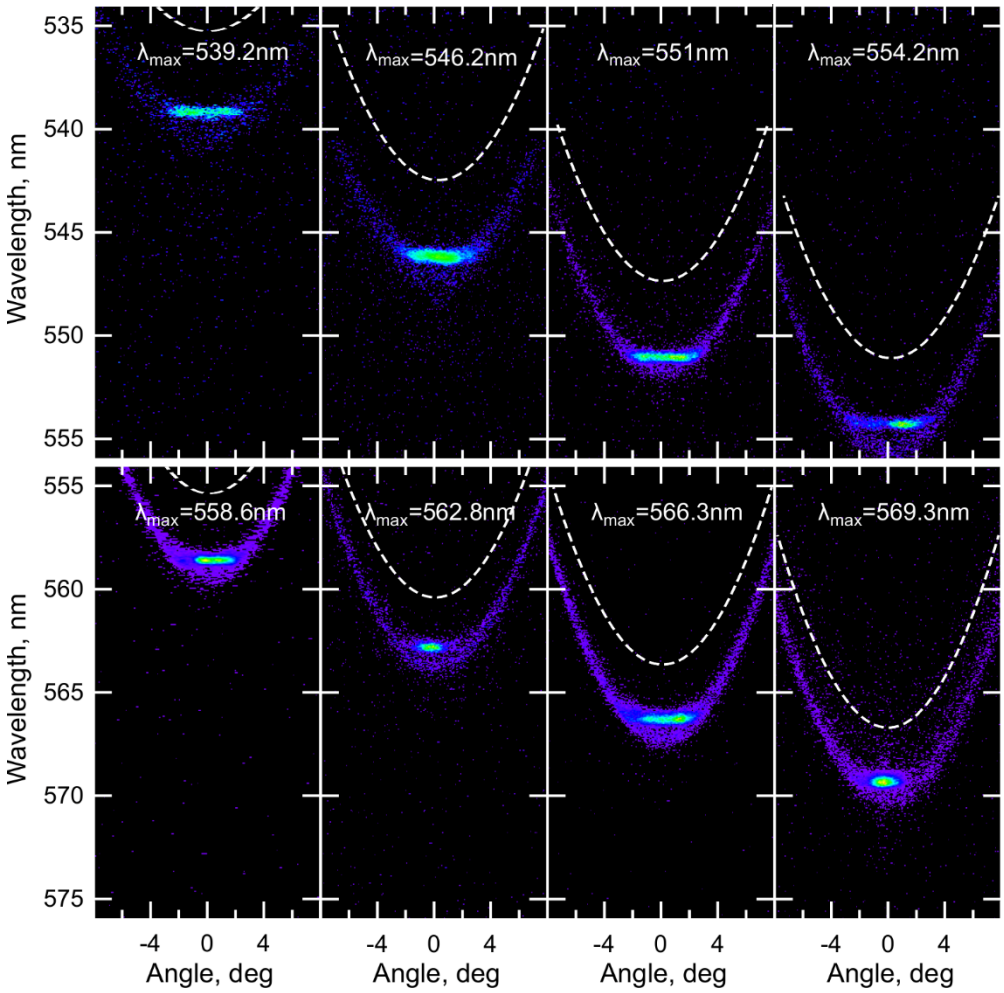

Figure S1 Superimposed below and above polariton lasing threshold dispersion images spanning the full spectral range reported in the main manuscript. Fluorescence from the lower polariton U-shaped dispersions identifies the linear regime, while the blue-shifted high intensity emission around normal incidence is indicative of polariton lasing. The white dashed lines correspond to the bare cavity mode.

On **Table S1** we present indicative values of the dependence of the effective refractive index n, the vacuum Rabi-splitting ħΩ, the exciton fraction $|X_{kII=0}|^2$ and photon fraction $|C_{kII=0}|^2$ for detunings spanning the whole spectrum under study here.

Detuning, eV	n	ħΩ, meV	$\|X_{kII=0}\|^2$	$\|C_{kII=0}\|^2$
-0.239	1.77	114	0.049	0.951
-0.195	1.79	116	0.070	0.930
-0.161	1.81	115	0.093	0.907
-0.127	1.84	112	0.125	0.875
Avg±Std	1.8±0.026	114±1.5		

Table S1 The refractive index n, vacuum Rabi splitting ħΩ, exciton and photon fractions $|X_{kII=0}|^2$ and $|C_{kII=0}|^2$ for each detuning realization. Average refractive index is 1.8, Rabi splitting – 114 meV. For less negative exciton-photon detuning, the exciton (photon) fraction naturally increases (decreases).

Threshold comparisons for ASE and polariton lasing:

To clarify the ASE threshold and compare it with the threshold of polariton lasing in a proper way, we have carried out new ASE measurements using a freshly prepared polystyrene/BODIPY-G1 film with the same thickness as in the microcavity (150 nm). The ASE threshold has been found at 6 mW of incident beam focused on the sample as a stripe (1470 x 80 μm) using 350 ps laser pulses at the excitation wavelength of 355 nm and 1 kHz repetition rate. Thus the incident pump fluence corresponding to the ASE threshold is equal to 5.2 mJ cm^{-2}. Taking into account the optical density (OD) of the film at 355 nm (OD=0.025) we obtain 290 uJ cm^{-2} of absorbed pump fluence at the ASE threshold. Meanwhile the polariton lasing occurs at 6 mJ cm^{-2} of the incident pump fluence at 400 nm. By taking into account the absorption of the film at 400 nm (OD=0.011) and the reflection losses on the first DBR (20%) we get an absorbed pump fluence for the polariton lasing of ~120 uJ cm^{-2}. Following this analysis, we can now compare the values of the absorbed pump fluences in the cavity and in the film. We find that the threshold for polariton lasing (120 uJ cm^{-2}) is ~2.5 times lower than for ASE (290 uJ cm^{-2}).